Carbon nanotube electrical-substitution cryogenic radiometer: initial results

N. A. Tomlin* and J. H. Lehman

National Institute of Standards and Technology (NIST), Boulder, Colorado 80305, USA
**Corresponding author: ntomlin@boulder.nist.gov*

Received November 14, 2012; accepted November 28, 2012;
posted December 3, 2012 (Doc. ID 179903); published January 10, 2013

A carbon nanotube cryogenic radiometer (CNCR) has been fabricated for electrical-substitution optical power measurements. The CNCR employs vertically aligned multiwall carbon nanotube arrays (VANTAs) as the absorber, heater, and thermistor, with a micromachined silicon substrate as the weak thermal link. Compared to conventional cryogenic radiometers, the CNCR is simpler, more easily reproduced and disseminated, orders of magnitude faster, and can operate over a wide range of wavelengths without the need for a receiver cavity. We describe initial characterization results of the radiometer at 3.9 K, comparing electrical measurements and fiber-coupled optical measurements from 50 μW to 1.5 mW at the wavelength of 1550 nm. We find the response to input electrical and optical power is equivalent to within our measurement uncertainty, which is currently limited by the experimental setup (large temperature fluctuations of the cold stage) rather than the device itself. With improvements in the temperature stability, the performance of the CNCR should be limited only by our ability to measure the reflectance of the optical absorber VANTA.

OCIS codes: 120.3930, 160.4236, 120.5630, 120.4800.

The electrical-substitution cryogenic radiometer (CR) is the basis for accurately measuring optical power at national metrology institutes around the world. The CR consists of several key components with separate functions: an optical absorber, thermistor, electrical heater, and weak thermal link [1]. Recently, vertically aligned multiwall carbon nanotube arrays (VANTAs) have been demonstrated to be the blackest substance known and have also been shown to have a temperature-dependent resistance [2–7]. We have taken advantage of the unique properties of VANTAs to combine several CR components in a novel carbon nanotube cryogenic radiometer (CNCR) that employs VANTAs as the absorber, heater, and thermistor. Compared to conventional CRs that are typically hand assembled, the CNCR is simpler, easily modified and duplicated, and has a response time at least 2 orders of magnitude faster.

The CNCR is fabricated from a double-side polished silicon wafer, which is lithographically patterned and micromachined using a Bosch process plasma etch to define the geometry [Fig. 1(a)]. The silicon leg that sets the weak thermal link has dimensions of 6.7 mm long, 2.6 mm wide, and 375 μm thick. We sent the micromachined silicon chip to a commercial company for VANTA growth, which consists of depositing 500 nm of SiO_2, 20 nm Al, oxidizing the Al to Al_2O_3, depositing 2 nm Fe, and chemical vapor deposition nanotube growth at 750°C for 2.5 min [4]. The VANTAs are ≈150 μm long and grown in 9 mm circles from the use of a shadow mask during the Fe deposition [Fig. 1(b)]. A second shadow mask is used to deposit 34 nm of Au at opposite sides of each VANTA. Electrical contact is made to each Au patch with silver-based conductive epoxy and ≈15 mm long Cu-clad NbTi wires. The base of the CNCR is clamped in a Cu sample holder and bolted to the second stage (≈4 K) of a pulse tube cooler in a dilution refrigerator.

Figure 1(c) shows the CNCR one-body thermal model, where we have neglected radiation loss and heat conduction along the electrical leads. The VANTA closest to the weak thermal link is used as the thermistor. The resistance of the thermistor is measured with a commercial lock-in amplifier, using a small AC excitation current in order to minimize self-heating.

The second VANTA performs the dual role of electrical heater and optical absorber. Input electrical power to the heater VANTA is determined using a commercial current source to set a stiff current bias, while the voltage is monitored. Input optical power is coupled to the heater VANTA using a standard 9 μm core, single-mode telecommunication fiber that is aligned at normal incidence to the center of the VANTA. The fiber tip has a 1550 nm antireflection coating that reduces the reflection from the tip to less than 0.3%. The distance between the fiber tip and VANTA is 9.1 mm, which gives a spot size diameter ($1/e^2$) of 1.7 mm. Known optical powers (≈ ± 0.5% due to unknown coupling and splice losses) are applied with a 1550 nm continuous wave fiber laser attenuated by two programmable fiber attenuators, which are calibrated using an optical switch and a National Institute of Standards and Technology (NIST)-calibrated power

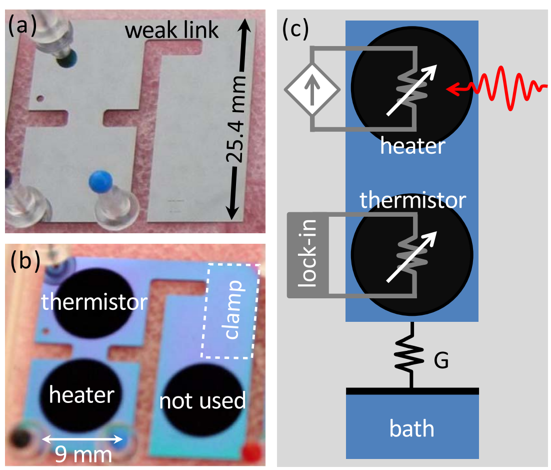

Fig. 1. (Color online) Micromachined silicon chip (a) before and (b) after VANTA growth. (c) One-body thermal model for the CNCR.

meter (Fig. 2). Unlike CRs, which typically use a trap or cavity design with multiple reflections to ensure near-unity optical absorption, the absorption of VANTAs is high enough that, for many applications, a cavity is unnecessary. Total hemispherical reflectance measurements of VANTAs have shown total reflectances ≤0.07% for visible wavelengths and 0.35% for 5–10 μm wavelengths [2,5].

During several cooldown and warmup cycles, the temperature of the commercial thermometer on the pulse tube stage (T) and the resistance of the thermistor VANTA (R) was monitored. The measured resistance as a function of temperature fits well to the Efros–Shklovskii modification of Mott variable range hopping theory given by $R = R_0 \exp(T_0/T)^{1/2}$, where we have fit $R_0 = 370\ \Omega$ and $T_0 = 93.5$ K (Fig. 3) [8]. The inset of Fig. 3 shows a thermistor sensitivity figure of merit, $\alpha = T/R \cdot dR/dT$.

Because of the extremely nonlinear change in resistance with temperature, the measured resistance of a VANTA is very sensitive to the spatial heating profile. This is the reason that two electrically separate VANTAs are required for the CNCR. The electrical and optical spatial heating profiles on the heater VANTA are quite different, which leads to different resistances for the same applied power. However, the thermistor VANTA is heated indirectly and thermalized by the phonons in the Si, so the resistance is only a function of temperature and independent of the method of heating.

To determine the thermal conductance of the silicon weak thermal link, we fit a power law of the form $P = K(T^3 - T_{\mathrm{bath}}^3)$, where P is the applied electrical power (50 μW to 1.5 mW), T is the temperature determined from the measured resistance and the Mott range hopping equation, $T_{\mathrm{bath}} = 3.9$ K is the bath temperature, and $K = 61\ \mu\mathrm{W/K}^3$ is the fit parameter. This gives a thermal conductance ($G = dP/dT = 3\ \mathrm{K}T^2$) of 2.8 mW/K and a thermal conductivity ($\kappa = G \cdot L/w/t$) of 19 W/K/m at 3.9 K, where w is the width, t the thickness, and L the length of the silicon thermal link.

To find the time constant of the CNCR, we used the optical switch to chop the optical power and fit an exponential to the thermistor rise and fall signal. This yielded a time constant of 6.7 ms.

To characterize the performance of the CNCR, electrical-substitution measurements were performed for applied optical powers of 50 μW to 1.5 mW at a base

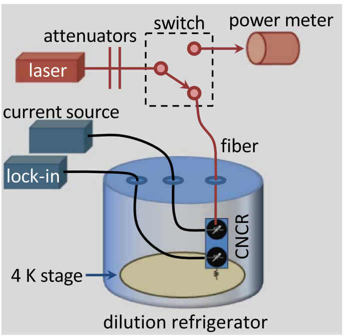

Fig. 2. (Color online) Simplified schematic of experimental apparatus.

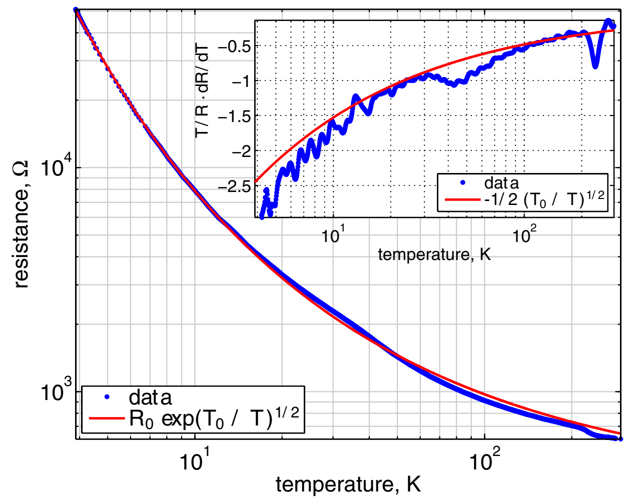

Fig. 3. (Color online) Thermistor VANTA resistance versus temperature. Solid red curve is the fit to the variable range hopping model. (Inset) Thermistor α versus temperature.

temperature of 3.9 K. For each applied optical power, the thermistor resistance was recorded repeatedly (seven times) and averaged; then the laser was blocked and the electrical power was varied while recording the thermistor resistance in order to match the optical resistance measurement. We define the response equivalence to be the ratio of the electrical power to optical power needed to match each resistance ($P_{\mathrm{elec}}/P_{\mathrm{opt}}$), plotted in Fig. 4(a). The mean response equivalence is 1.003. A sliding window (nearest neighbor, 20 points) was used to determine the standard deviation ($k = 2$) of the response equivalence, which decreases with increasing power down to ±0.3% [Fig. 4(b)]. This response equivalence standard deviation, along with the uncertainty in the measurement of the optical power, means that the response of the CNCR to electrical and optical power is the same, within the uncertainty of the present measurements. Because the CNCR was attached directly

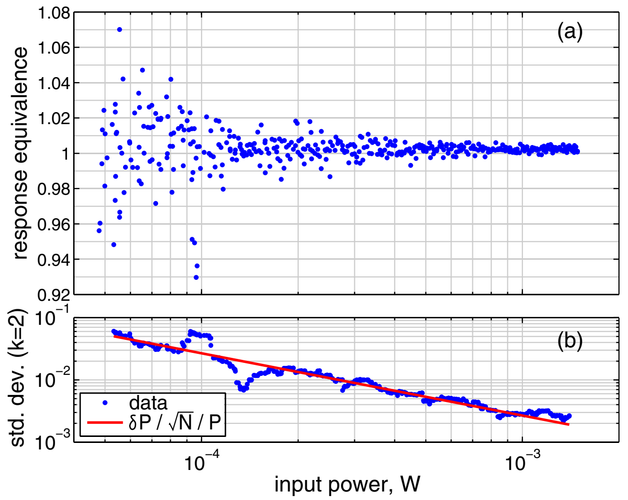

Fig. 4. (Color online) (a) CNCR response equivalence versus input power. (b) Standard deviation ($k = 2$) versus input power obtained from a sliding window on the data in (a). Solid line is the predicted standard deviation expected from the variation in bath temperature.

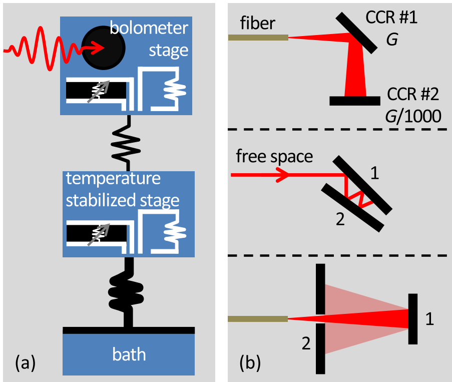

Fig. 5. (Color online) (a) Thermal model for a future improved-performance CNCR. (b) Schematic of potential trap designs utilizing two CNCRs with different strength thermal links (G).

to the pulse tube stage with no temperature stabilization, the bath temperature fluctuated by 5 mK peak to peak (sine wave at the pulse tube frequency of 1.425 Hz), which is equivalent to a standard deviation power fluctuation at the thermistor of $\delta P = G \cdot \delta T = 10\ \mu\text{W}$ ($k = 2$). The solid line in Fig. 4(b) is the expected standard deviation of the response equivalence due to the temperature fluctuation, using $\delta P/\sqrt{N}/P$, where $N = 14$ is the number of resistance measurements averaged. The plot shows that the uncertainty in the measurement is dominated by the bath temperature fluctuation.

The present CNCR was designed more for characterization purposes rather than performance: the weak link was made to be robust (large G) for ease of handling, and a VANTA was used as the electrical heater for simplicity and to provide the opportunity to swap roles of the two VANTAs. Some simple modifications that would increase the performance of a future CNCR are adding an additional weak link to act as the integrated temperature stabilized platform, adding a resistive thin film electrical heater to reduce the uncertainties due to a nonlinear electrical heater, reducing the spacing between leads on the thermistor VANTA in order to lower the resistance for higher accuracy readout, and using thin film superconducting wiring for electrical contact instead of macroscopic NbTi wiring [Fig. 5(a)]. Additionally, the lithographic design of the CNCR makes it easy to modify any element of the design. For example, the weak link G can easily be reduced by more than a factor of 500 or increased by adding a metal layer.

If the bath temperature fluctuations were made negligible, the theoretical noise of the CNCR would be dominated by thermal fluctuation noise from the weak link, which would be a noise equivalent power of approximately $\sqrt{4k_B \mathrm{G}\mathrm{T}^2} \simeq 10^{-12}\ \mathrm{W}/\sqrt{\mathrm{Hz}}$ [9]. This means that a half second integration time would yield a noise performance nearly 7 orders of magnitude better than the measurements presented in this Letter. The ultimate accuracy of the CNCR should be limited only by our ability to measure the reflectance of the nanotube array, which is currently $\pm 0.3\%$ for wavelengths below 10 μm [5]. While the CNCR is limited to a planar absorber, two CNCRs could be combined in a trap configuration in order to reduce the uncertainty on the reflectivity [Fig. 5(b)]. The flexibility of the CNCR allows for more exotic trap designs where, for example, the second CNCR has a G much lower than the first to make it sensitive to the extremely low reflection off the first CNCR.

In conclusion, we have demonstrated promising initial results of a novel electrical-substitution CR. Compared to traditional CRs, the use of VANTAs and a lithographically patterned heat link make the CNCR simpler, faster, and more easily modified and duplicated. While the present results are more a proof of principle, simple changes will greatly improve future CNCR performance.

References

1. J. E. Martin, N. P. Fox, and P. J. Key, Metrologia **21**, 147 (1985).
2. Z. Yang, L. Ci, J. A. Bur, S. Lin, and P. M. Ajayan, Nano Lett. **8**, 446 (2008).
3. K. Mizuno, J. Ishii, H. Kishida, Y. Hayamizu, S. Yasuda, D. N. Futaba, M. Yumura, and K. Hata, Proc. Natl. Acad. Sci. USA **106**, 6044 (2009).
4. J. Lehman, A. Sanders, L. Hanssen, B. Wilthan, J. Zeng, and C. Jensen, Nano Lett. **10**, 3261 (2010).
5. C. J. Chunnilall, J. H. Lehman, E. Theocharous, and A. Sanders, Carbon **50**, 5348 (2012).
6. M. E. Itkis, F. Borondics, A. Yu, and R. C. Haddon, Science **312**, 413 (2006).
7. A. Okamoto, I. Gunjishima, T. Inoue, M. Akoshima, H. Miyagawa, T. Nakano, T. Baba, M. Tanemura, and G. Oomi, Carbon **49**, 294 (2011).
8. Z. Khan, S. Husain, and M. Husain, Current Nanosci. **6**, 626 (2010).
9. J. C. Mather, Appl. Opt. **21**, 1125 (1982).